Journal of Atmospheric and Solar-Terrestrial Physics 72 (2010) 1–6

Contents lists available at ScienceDirect

Journal of Atmospheric and Solar-Terrestrial Physics

journal homepage: www.elsevier.com/locate/jastp

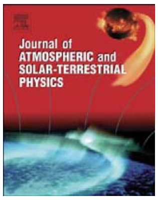

On the modulation of intensity of Alfvén resonances before earthquakes: Observations and model

V. Grimalsky [a,*], A. Kotsarenko [b,**], S. Pulinets [c], S. Koshevaya [a], R. Perez-Enriquez [b]

[a] UAEM, CIICAp, Cuernavaca, Morelos, Z.P. 62209, Mexico
[b] Center for Geoscience in Juriquilla, UNAM, P.O. 1-742, Queretaro, Z.P. 76001, Mexico
[c] Institute for Geophysics, UNAM, Mexico D.F., Z.P. 04510, Mexico

ARTICLE INFO

Article history:
Received 16 December 2008
Received in revised form
6 July 2009
Accepted 27 September 2009
Available online 12 October 2009

Keywords:
Ionosphere Alfvén Resonator
Seismogenic coupling
Modulation of ionosphere parameters

ABSTRACT

Modulation of magnetic components of ULF Alfvén wave (f=0.02–2 Hz), which is incident from the magnetosphere to the Earth's surface, is considered. This modulation is due to variations of electron and ion concentrations within the ionosphere F-layer caused by acoustic-gravity waves or internal gravity waves of ULF (0.0005–0.02 Hz) range. The maximum modulation of the magnetic field at the Earth's surface takes place when maximum variations of the electron concentration are observed at altitudes 225–275 km. The modulation is more essential when the inclination angle of the geomagnetic field is $\geq 50^\circ$. The 20% modulation of the electron concentration results in the magnetic field modulation at the Earth's surface of 30–40%. At the frequencies $f \sim 1$ Hz there exists the resonant modulation when in the narrow (~ 0.1 Hz) frequency range the modulation increases sharply. The results can explain the ground-based observations of generation of the seismo-related ULF magnetic perturbations.

1. Introduction

Recently, generation of the seismo-related Ultra Low Frequency (ULF, 0.1–10 Hz) magnetic perturbations, locally generated geomagnetic pulsations, changes in regular resonant structures were confirmed experimentally by different ground-based observations (Kotsarenko et al., 2004, 2005, 2007). In order to give a possible explanation we link mentioned phenomena with a modification of the parameters of the ionosphere (such as electron density and the temperature), which is regularly detected during satellite observations over earthquake preparation areas (Gousheva et al., 2008; Sarkar et al., 2007). Namely, both fundamental mechanisms of the lithosphere–atmosphere–ionosphere coupling, i.e. coupling through the changes in the atmospheric electricity produced as result of integrated ionization from the increased radon emanation (Pulinets and Boyarchuk, 2004) and the conversion of atmospheric acoustic-gravity waves (AGW) and internal gravity waves (IGW) in the lower ionosphere (Hayakawa and Molchanov, 2002; Molchanov, 2004) can lead to the modulation of the ionosphere parameters, creating transparency of the ionosphere for a passage of the Alfvén waves, which go from the magnetosphere down to the Earth's surface (Guglielmi and Pokhotelov, 1996; Guglielmi et al., 2006). We mention that IGW may reach the altitudes of 300–500 km, whereas AGW at frequencies 0.005–0.02 Hz may reach the altitudes of 200–300 km (Hayakawa, 1999; Koshevaya et al., 2005).

In this paper, we consider the explanation of observed magnetic perturbations by modulation of electrodynamic properties of the atmosphere F-layer. In literature there are alternative explanations of this phenomenon, due to strong electric field formation in the lower ionosphere (Chmyrev et al., 2008; Sorokin et al., 2001, 2003, 2005a, 2005b). Such an alternative explanation is as follows. Seismic activity is accompanied by emanation of soil gases into the atmosphere. These gases transfer positive and negative charged aerosols. Atmospheric convection of charged aerosols forms external electric current, which works as a source of perturbation in the atmosphere–ionosphere electric circuit. DC electric field can be generated by this current. In turn, DC electric field leads to electrodynamic instabilities. Interaction of the background electromagnetic ULF waves with such structure leads to an excitation of polarization currents and generation of narrow band gyrotropic waves at the 0.1–10 Hz frequency range in the ionosphere. The magnetic field of these waves can be observed on the ground (Sorokin et al., 2003).

We mention that our explanation does not need any additional instability in the ionosphere and it seems more direct that one proposed in cited above papers.

---

[*] Corresponding author. Tel./fax: +52 777 3297084.
[**] Corresponding author.
E-mail addresses: v_grim@yahoo.com (V. Grimalsky), kotsarenko@geociencias.unam.mx (A. Kotsarenko).

1364-6826/$ - see front matter © 2009 Published by Elsevier Ltd.
doi:10.1016/j.jastp.2009.09.017

2. Observations

An analysis of geomagnetic and telluric data, measured at the station PRK (Parkfield, ULF fluxgate 3-axial magnetometer) one week before (including) the day of major EQ (EarthQuake, Ms = 6.0, 28-SEP-2004, 17:15:24) near Parkfield, California, USA, is presented. The spectral analysis reveals the ULF geomagnetic disturbances observed on the day before the event, September, 27, at 15:00–20:00 by UT, and on the day of the EQ, September, 28, at 11:00–19:00, see Fig. 1. The filtering in the corresponding

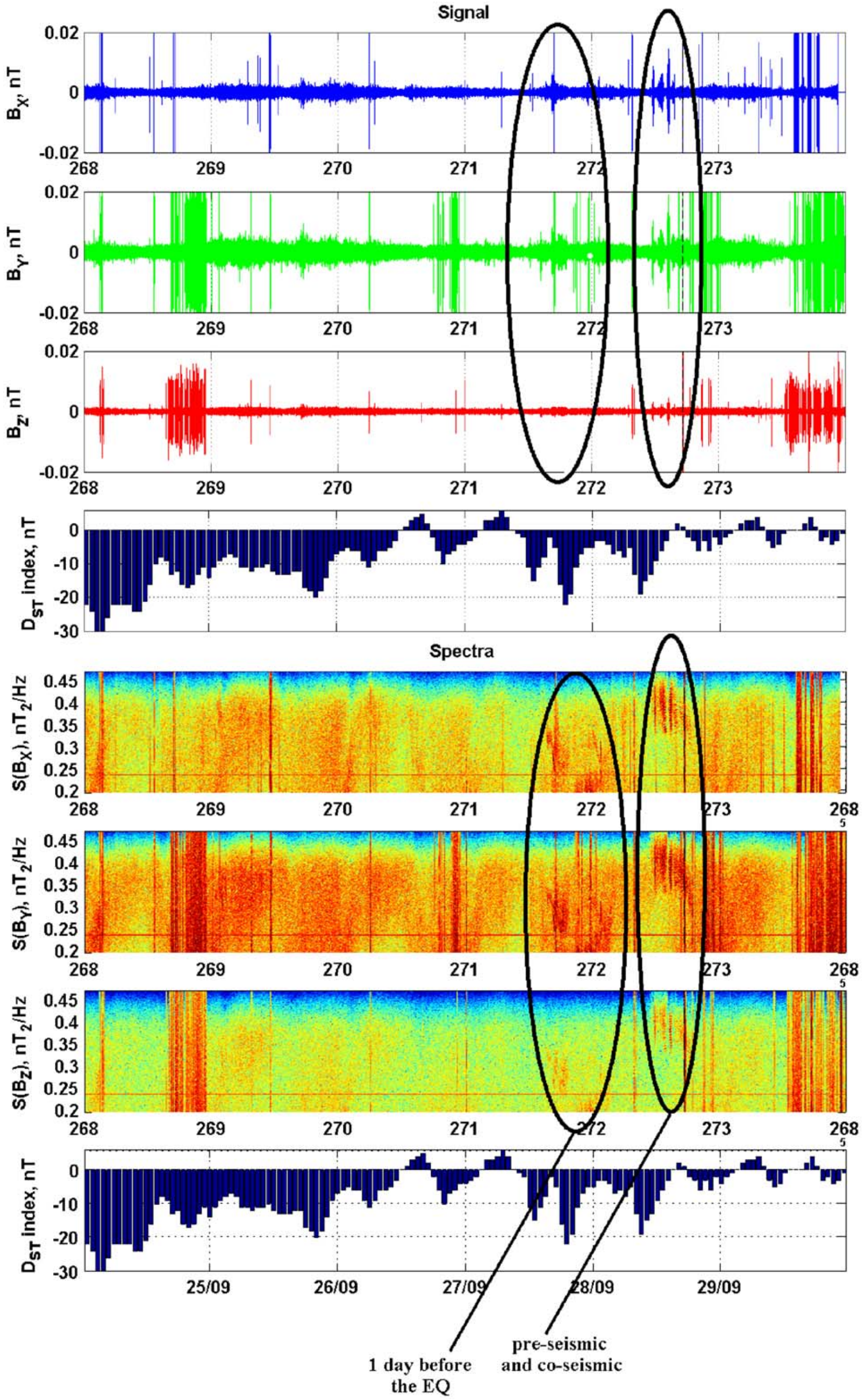

Fig. 1. Geomagnetic signals, 3 magnetic components and their spectra observed during September 24–28, 2004. Reference panels (4 and 8): D_{st} index of the geomagnetic activity. EQ moment is indicated by black dashed line. Short-time precursors are observed at the day before the EQ, September 27 (area indicated by the first ellipse). Near-time, co-seismic and post-seismic signals are observed at the EQ day (the second ellipse).

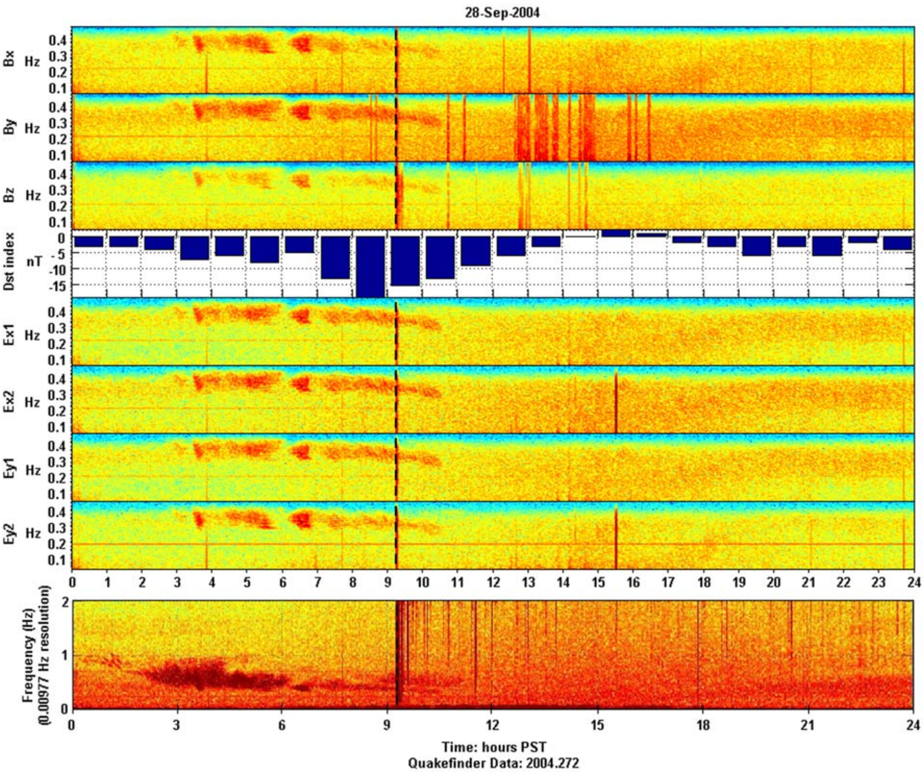

Fig. 2. First 3 panels: magnetic components. 4th panel: D_{st} index. Panels 4–7: electric components (2 X- and 2 Y- dipoles). Lower panel: results obtained by Quake Finder research group. EQ moment is indicated by black dashed line.

frequency band f=0.25–0.5 Hz gives the following estimations of the amplitudes of the signals: up to 20 pT for the magnetic channels and 1.5 μV/km for the telluric ones.

Observed phenomena occur under quiet geomagnetic conditions ($|D_{st}| < 20$ nT); a revision of the referent stations data situated far away from the EQ epicenter (330 km) does not reveal any similar effect. Moreover, the Quake Finder research group received very similar results (ELF range instrumentation, placed about 50 km from the EQ epicenter) for the day of the EQ (Bleier, 2005).

A comparative analysis of the mentioned two stations (Fig. 2) shows that the lower-frequency part of the ULF burst was observed, which was localized in the eigenfrequencies of the Alfvén resonances in the frequency range 0.25–1 Hz, generated 9 h before the earthquake.

3. Model and basic equations

Propagation of EMW of ULF and ELF ranges in the magnetosphere, ionosphere, and atmosphere is considered, see Fig. 3. A general case of oblique incidence of the Alfvén wave from the magnetosphere is investigated. The system is assumed as uniform in (XY) plane. The curvature of the Earth's surface is neglected, because the condition $L_z \ll R_E$=6400 km is valid. Basic volume equations are:

$$\vec{E},\vec{H} \sim \exp(i\omega t - ik_x x); \quad \omega = const, \quad k_x = const;$$
$$k_0 \equiv \frac{\omega}{c}: \quad \nabla(\nabla\cdot\vec{E}) - \Delta\vec{E} = k_0^2\vec{D}; \quad \vec{D} = \widehat{\varepsilon}(\omega,z)\vec{E}; \quad \nabla\times\vec{E} = -ik_0\vec{H} \tag{1}$$

Here k_x=$k_0(\varepsilon'_1)^{1/2}\sin\Theta$ is the horizontal component of the wave vector of the EM wave (k_y=0); Θ is the incidence angle, which coincides with the inclination angle of the geomagnetic field $\boldsymbol{H_0}$.

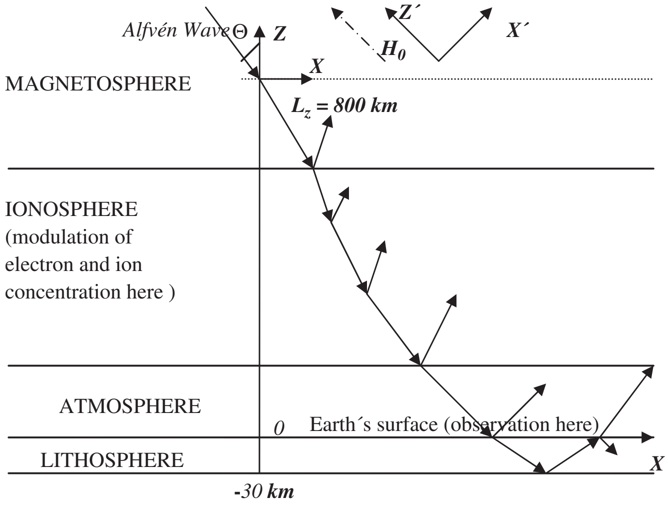

Fig. 3. Passage of the Alfvén wave through the magnetosphere and ionosphere to the Earth's surface. The coordinate frame (X, Y, Z) is associated with the Earth's surface, (X', Y, Z') is associated with the geomagnetic field H_0.

From (1), one can derive the equations for E_x, E_y components:

$$\frac{\partial}{\partial z}\left(\frac{\varepsilon_{33}(\partial E_x)/(\partial z)}{\varepsilon_{33}-(k_x^2)/(k_0^2)}\right) - ik_x\frac{\partial}{\partial z}\left(\frac{\varepsilon_{31}E_x}{\varepsilon_{33}-(k_x^2)/(k_0^2)}\right)$$
$$-ik_x\varepsilon_{13}\left(\frac{(\partial E_x)/(\partial z)}{\varepsilon_{33}-(k_x^2)/(k_0^2)}\right) \quad -ik_x\frac{\partial}{\partial z}\left(\frac{\varepsilon_{32}E_y}{\varepsilon_{33}-(k_x^2)/(k_0^2)}\right)$$
$$+k_0^2\left(\varepsilon_{11}-\frac{\varepsilon_{13}\varepsilon_{31}}{\varepsilon_{33}-(k_x^2)/(k_0^2)}\right)E_x + k_0^2\left(\varepsilon_{12}-\frac{\varepsilon_{13}\varepsilon_{32}}{\varepsilon_{33}-(k_x^2)/(k_0^2)}\right)E_y = 0;$$

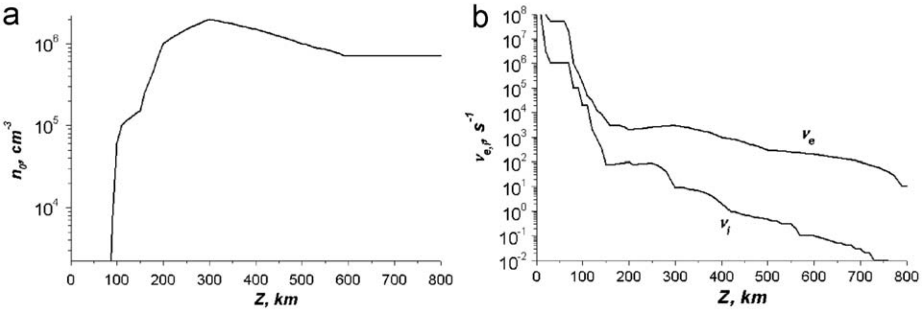

Fig. 4. Dependencies of electron concentration (a) and collision frequencies for electrons and ions (b), used in simulations, on the height *z*.

$$\frac{\partial^2 E_y}{\partial z^2} - ik_x\varepsilon_{23}\left(\frac{(\partial E_x)/(\partial z)}{\varepsilon_{33}-(k_x^2)/(k_0^2)}\right) + k_0^2\left(\varepsilon_{21}-\frac{\varepsilon_{23}\varepsilon_{31}}{\varepsilon_{33}-(k_x^2)/(k_0^2)}\right)E_x + k_0^2\left(\varepsilon_{22}-\frac{\varepsilon_{23}\varepsilon_{32}}{\varepsilon_{33}-(k_x^2)/(k_0^2)}\right)E_y - k_x^2 E_y = 0; \quad (2)$$

$$H_x = -\frac{i}{k_0}\frac{\partial E_y}{\partial z};$$

$$H_y = \frac{i}{k_0}\left(\frac{\varepsilon_{33}}{\varepsilon_{33}-(k_x^2)/(k_0^2)}\frac{\partial E_x}{\partial z} - ik_x\frac{\varepsilon_{31}E_x}{\varepsilon_{33}-(k_x^2)/(k_0^2)} - ik_x\frac{\varepsilon_{32}E_y}{\varepsilon_{33}-(k_x^2)/(k_0^2)}\right);$$

$$H_z = \frac{k_x}{k_0}E_y$$

The boundary conditions at $z=L_z$ have been obtained from the condition that only the incident Alfvén wave (at $z>L_z$) exists:

$$\frac{\partial E_x}{\partial z} + ik_{3z}E_x = -i(k_{1z}-k_{3z})E_{ix}; \quad \frac{\partial E_y}{\partial z} - ik_{2z}E_y = -2ik_{2z}E_{iy};$$

$$k_{1z} = k_{z'}\cos\Theta; \quad k_{3z} = -k_{z'}\left(\cos\Theta + \frac{2(\varepsilon'_3-\varepsilon'_1)\sin^2\Theta\cos\Theta}{\varepsilon'_3\cos^2\Theta+\varepsilon'_1\sin^2\Theta}\right);$$

$$k_{2z} = k_{z'}\cos\Theta; k_{z'} = k_0(\varepsilon'_1)^{1/2}; \quad k_{x'} \approx 0. \quad (3)$$

Here E_{ix}, E_{iy} are amplitudes of incident waves of different polarizations. Under the propagation in the high magnetosphere ($z>800$ km), the Alfvén wave possesses small diffraction whereas the fast magnetosonic wave is subject to strong diffraction, so it is possible to approximate that in (3) E_{ix}, E_{iy} are the amplitudes of the Alfvén wave. The Alfvén wave can be excited by external sources within the magnetosphere over the region $z>800$ km. Here we consider the simplest case when the wave vector of the incident wave is directed along the geomagnetic field H_0 ($k_{x'}\approx 0$). The amplitudes E_{ix}, E_{iy} are independent in this case. Therefore, propagation of ULF-ELF electromagnetic wave within the magnetosphere, ionosphere, atmosphere, and lithosphere has been simulated within the full-wave method, where reflections at the boundaries of the horizontal layers have been taken into account automatically.

Generally (for magnetosphere and ionosphere), the expression for the effective dielectric tensor is (Guglielmi and Pokhotelov, 1996):

$$\widehat{\varepsilon'} = \begin{pmatrix} \varepsilon'_1 & ig & 0 \\ -ig & \varepsilon'_1 & 0 \\ 0 & 0 & \varepsilon'_3 \end{pmatrix}; \quad \varepsilon_{lm} = \alpha_{ll'}\alpha_{mm'}\varepsilon'_{l'm'}$$

$$\varepsilon'_1 = 1 - \frac{\omega_{pe}^2(\omega - i\nu_e)}{\omega((\omega-i\nu_e)^2-\omega_{He}^2)} - \frac{\omega_{pi}^2(\omega-i\nu_i)}{\omega((\omega-i\nu_i)^2-\omega_{Hi}^2)};$$

$$\varepsilon'_3 = 1 - \frac{\omega_{pe}^2}{\omega(\omega-i\nu_e)} - \frac{\omega_{pi}^2}{\omega(\omega-i\nu_i)};$$

$$g = \left(\frac{\omega_{pe}^2\omega_{He}}{\omega((\omega-i\nu_e)^2-\omega_{He}^2)} - \frac{\omega_{pi}^2\omega_{Hi}}{\omega((\omega-i\nu_i)^2-\omega_{Hi}^2)}\right);$$

$$\omega_{pe}^2 = \frac{4\pi e^2 n_0}{m_e}, \quad \omega_{pi}^2 = \frac{4\pi e^2 n_0}{m_i}, \quad \omega_{He} = \frac{eH_0}{m_e c}, \quad \omega_{Hi} = \frac{eH_0}{m_i c}.$$

Here $\alpha_{ll'}$ are the elements of the matrix of rotation from ($X'\,YZ'$) frame to (XYZ) one.

In the magnetosphere ($z>600$ km), gyrotropy is absent: $g=0$ (Guglielmi and Pokhotelov, 1996). In our simulations, it has been assumed that the geomagnetic field varies from H_0=0.4 Oe (z=0) to H_0=0.3 Oe (z=800 km). The results are tolerant to small variations of the geomagnetic field. The parameters of the ionosphere and the magnetosphere used in simulations are given in Fig. 4.

4. Simulations

We have calculated the efficiency of the modulation of the Alfvén wave at the frequencies f=0.02–1.6 Hz ($\omega=2\pi f$=0.1–10 s^{-1}), which passes from the magnetosphere ($z>600$ km) down to the ionosphere and, the to the Earth's surface and the lithosphere. The set of equations for the electric field components $E_{x,y}$ has been solved numerically. The boundary conditions are as follows. At z=800 km the amplitude of the downgoing Alfvén wave is assumed as constant (specifically, the field of the Alfvén resonator (Fedorov et al., 2006); at $z=-30$ km (in the deep lithosphere) there is $E_{x,y}$=0. The conductivity of the lithosphere is $\sigma=10^3$–10^5 s^{-1} (Guglielmi and Pokhotelov, 1996).

We assume that under preparation of strong earthquakes the acoustic-gravity waves (AGW) and internal gravity waves (IGW) of ULF frequency range (0.0005–0.02 Hz) can be excited, which propagate from the Earth's surface upwards and penetrate into E and F-layers of the ionosphere (Guglielmi et al., 2006). At the Earth's surface, the magnitude of AGW and IGW are small. Nevertheless, these waves possess relatively weak dissipation and their amplitudes increase with the height z (Guglielmi and Pokhotelov, 1996). Within the F-layer, AGW and IGW lead to a variation (modulation) of the concentration of electrons and ions (Hayakawa, 1999). Namely, the penetration of AGW and IGW on the altitudes 200–300 km results in the vertical displacement of the ionosphere layers of 10–50 km. This variation results in changes of a transparency of ULF EM waves, passing through the ionosphere from the magnetosphere, at frequencies higher that the frequencies of AGW and IGW. Note also that the authors (Sorokin et al., 2001) mentioned that an elevation of the F-layer maximum, a decrease of electron density in the maximum of this layer and a growth of light-ion density in the upper ionosphere can be also due to the modification of DC electric field in the ionosphere. This modification is connected with increase of atmospheric radioactivity and injection of charged aerosols into the atmosphere.

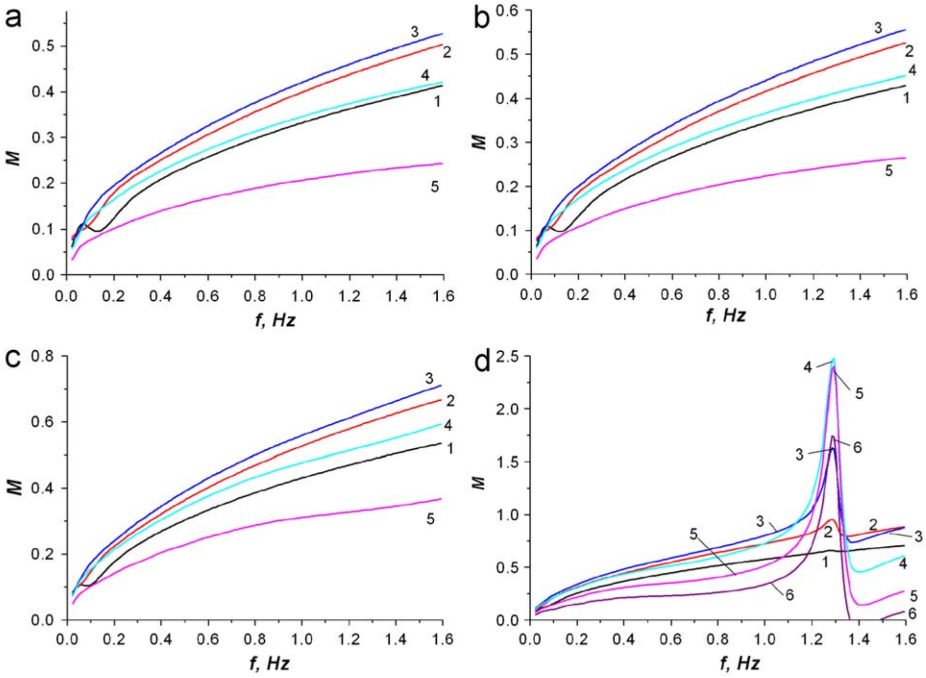

Fig. 5. Dependence of modulation of h_x component of the magnetic field at the Earth's surface on frequency. Part a) is for the incidence angle $\Theta=0^\circ$, (b) $\Theta=30^\circ$, (c) $\Theta=60^\circ$, (d) $\Theta=75^\circ$. The parameter of modulation is $m=-0.2$. Curve 1 is for $z_1=200$ km, 2 is for $z_1=225$ km, 3 is for $z_1=250$ km, 4 is for $z_1=275$ km, 5 is for $z_1=300$ km, 6 is for $z_1=325$ km. The E_x polarization of the incident wave, $z_0=30$ km for all cases.

A modulation of electron (and ion) concentration of the ionosphere plasma has been considered as: $n(z)=n_0(z)\times(1+m\times\exp(-((z-z_1)/z_0)^2))$, where the modulation degree is $|m|\ll 1$; $n_0(z)$ is the unperturbed concentration. It is assumed that the region of variation of electron concentration is uniform in the (X, Y) plane. A possible difference from this model is discussed briefly below.

The modulation of the magnetic field at the Earth's surface is estimated as $M=(H-H_0)/H_0$, where H_0 is the amplitude of the magnetic field at the Earth's surface in the absence of the variations within the F-layer, H is the amplitude of the magnetic field calculated with the variations. The biggest component of the magnetic field has been taken into consideration. Both in the case of E_x polarization and of E_y one of the incident EM wave, it is H_x.

The results of simulations are given in Figs. 5–7. A high (uniform) modulation exists in a wide range of frequencies. It is expressed when the incidence angle is great: $\Theta=50$–80°. It has been obtained that the 5–20% modulation of the concentration of the ion and electron concentrations at the heights $z\approx 250$ km can lead to the 20–50% modulation of the amplitude of the variable magnetic field at the Earth's surface ($z=0$) at the frequencies $f=0.02$–1.6 Hz. The effect depends weakly on the conductivity σ of the lithosphere.

At the angles of incidence $\Theta>60^{\mathrm{o}}$ the resonant modulation can occur. Namely, in some narrow frequency band near the frequency $f\sim 1$ Hz, a sharp increase of the modulation degree M takes place in the case of E_x polarization of the incident wave. The modulation M can be 3–5 times higher there. A possible explanation of such a resonant behavior is as follows. At great angles of incidence of the Alfvén wave from the magnetosphere to the ionosphere, the EM wave is subject to the internal wave reflection in the regions of higher effective dielectric permittivity (F-layer). A decrease of the electron concentration in F-layer leads to a sharp (exponential) increase of the transparency. When comparing with the observation results, it is possible to conclude that in our case a non-resonant modulation at lower frequencies was detected.

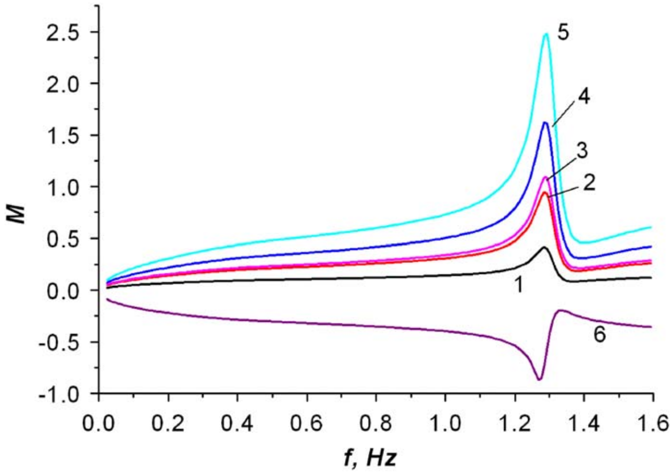

Fig. 6. Dependence of modulation of h_x component of the magnetic field at the Earth's surface on frequency, the incidence angle is $\Theta=75^\circ$: curve 1 is for $m=-0.05$, $z_0=30$ km, 2 is for $m=-0.1$, $z_0=30$ km, 3 is for $m=-0.15$, $z_0=30$ km, 4 is for $m=-0.2$, $z_0=15$ km, 5 is for $m=-0.2$, $z_0=30$ km, 6 is for $m=0.2$, $z_0=30$ km; For all cases, $z_1=275$ km, E_x polarization of the incident wave.

The results of effective modulation of ULF-ELF waves have been confirmed also when the beam of Alfvén waves of finite transverse sizes has been considered. Under the oblique incidence $\Theta>60^{\mathrm{o}}$ and the finite transverse size of the incident beam of about 600 km, the transverse size of the 'spot' of the electromagnetic wave along X-axis is of about 1500 km. This can explain the localization of modulation effect of ULF magnetic field at the Earth's surface, namely, the fact that the modulation of ULF magnetic field was not observed at the distances $\sim$400 km from the observation point.

Therefore, an influence of the lithosphere–ionosphere coupling mechanisms on the concentration of carriers in F-layer of the ionosphere could lead to observable effects at the Earth's surface.

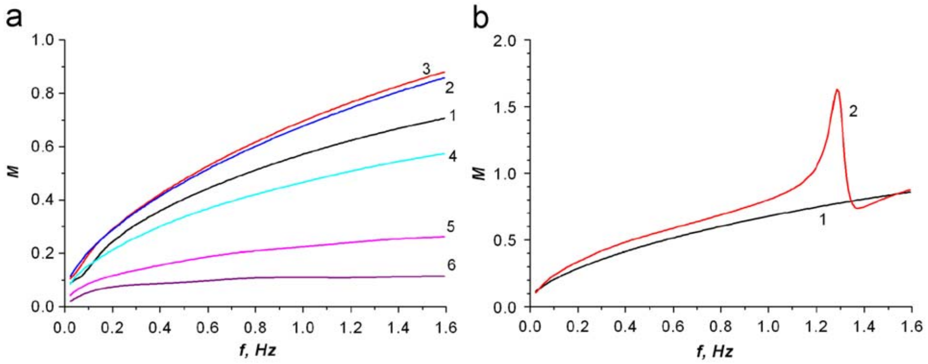

Fig. 7. Dependence of modulation of the h_x magnetic field component at the Earth's surface on frequency, $\Theta=75^\circ$, $m=-0.2$, $z_0=30$ km. Part (a) is the modulation for E_y polarization of the incident wave (curve 1 is for $z_1=200$ km, 2 is for $z_1=225$ km, 3 is for $z_1=250$ km, 4 is for $z_1=275$ km, 5 is for $z_1=300$ km, 6 is for $z_1=325$ km). Part (b) is a comparison of modulation degree of h_x component for E_y polarization of the incident wave (curve 1) and modulation of h_x component for E_x polarization of the incident wave (curve 2), $z_1=250$ km, $z_0=30$ km.

5. Conclusions

The change of the electron concentration in F-layer of the ionosphere due to passage of acoustic-gravity waves and internal gravity waves, which go upwards in the preparation period before earthquakes and can lead to essential modulation of the ULF magnetic fields at the Earth's surface. These magnetic fields are produced by Alfvén waves, which penetrate from the magnetosphere to the Earth's surface. In the frequency range 0.2–2 Hz this modulation is 2 times higher than the variation of the electron concentration at the heights 225–275 km, in the case when the incidence angle of the Alfven wave is 50° and more. In the narrow frequency range of the width 0.1 Hz in the vicinity of the frequency $f\sim 1$ Hz the resonant modulation can occur, where the modulation of the magnetic field is 3–5 times higher than out of this region.

Acknowledgements

This work was partially supported by the internal UNAM foundation DGAPA (scientific projects PAPIIT IN120808). The authors are grateful to M. Johnston for providing us with the Parkfield Site data.

References

Bleier, T., 2005. ELF Magnetic Field Monitoring of the San Simeon M6.4 Quake From Both QuakeSat and a Ground Network. Proceedings of International Workshop on Seismo Electromagnetics, Tokyo, Japan, March . 〈http://quakefinder.com/frontPage/reference/L3-3%20Bleier.pdf〉.

Chmyrev, V.M., Sorokin, V.M., Shklyar, D.R., 2008. VLF transmitter signals as a possible tool for detection of seismic effects on the ionosphere. Journal of Atmospheric and Solar-Terrestrial Physics 70 (16), 2053–2060.

Fedorov, E., Schekotov, A.Ju., Molchanov, O.A., Hayakawa, M., Surkov, V.V., Gladichev, V.A., 2006. An energy source for the mid-latitude IAR: world thunderstorm centers, nearby discharges or neutral wind fluctuations? Physics and Chemistry of the Earth 31 (4), 462–468.

Gousheva, M.N., Glavcheva, R.P., Danov, D.L., Hristov, P.L., Kirov, B.B., Georgieva, K.Y., 2008. Electric field and ion density anomalies in the mid latitude ionosphere: possible connection with earthquakes?. Advances in Space Research 42, 206–212.

Guglielmi, A.V., Pokhotelov, O.A., 1996. Geoelectromagnetic Waves. Institute of Physics Publ., Bristol and Philadelphia.

Guglielmi, A., Potapov, A., Tsegmed, B., Hayakawa, M., Dovbnya, B., 2006. On the earthquake effects in the regime of ionospheric Alfvén resonances. Physics and Chemistry of the Earth 31 (4), 469–472.

Hayakawa, M. (Ed.), 1999. Atmospheric and Ionospheric Electromagnetic Phenomena Associated with Earthquakes. TERRAPUB, Tokyo.

Hayakawa, M., Molchanov, O. (Eds.), 2002. Seismo Electromagnetics Lithosphere–Atmosphere–Ionosphere Coupling. TERRAPUB, Tokyo.

Kotsarenko, A., Perez Enriquez, R., Lopez Cruz-Abeyro, J.A., Koshevaya, S., Grimalsky, V., 2004. Analysis of the ULF electromagnetic emission related to seismic activity, Teoloyucan geomagnetic station, 1998–2001. Natural Hazards and Earth System Sciences (NHESS) 4 (5–6), 679–684.

Kotsarenko, A., Molchanov, O., Perez Enriquez, R., Lopez Cruz-Abeyro, J.A., Koshevaya, S., Grimalsky, V., Kremenetsky, I., 2005. Possible seismogenic origin of changes in the ULF EM resonant structure observed at Teoloyucan geomagnetic station, Mexico, 1999–2001. Natural Hazards and Earth System Sciences (NHESS) 5 (5), 711–715.

Kotsarenko, A., Perez Enriquez, R., Lopez Cruz-Abeyro, J.A., Koshevaya, S., Grimalsky, V., Yutsis, V., Kremenetsky, I., 2007. ULF geomagnetic anomalies of possible seismogenic origin observed at Teoloyucan station, Mexico, in 1999–2001: intermediate and short-time analysis. Tectonophysics 431 (1–4), 249–262.

Koshevaya, S.V., Grimalsky, V.V., Perez-Enriquez, R., Kotsarenko, A.N., 2005. Increase of the transparency for cosmic radio waves due to the decrease of density of the ionosphere caused by acoustic waves. Physica Scripta 72 (2), 91–99.

Molchanov, O.A., 2004. On the origin of low- and middler-latitude ionospheric turbulence. Physics and Chemistry of the Earth 29 (4–9), 559–566.

Pulinets, S.A., Boyarchuk, K.A., 2004. Ionospheric Precursors of Earthquakes. Springer, Berlin, Heidelberg, New York.

Sarkar, S., Gwal, A.K., Parrot, M., 2007. Ionospheric variations observed by the DEMETER satellite in the mid-latitude region during strong earthquakes. Journal of Atmospheric and Solar-Terrestrial Physics 69 (13), 1524–1540.

Sorokin, V.M., Chmyrev, V.M., Yaschenko, A.K., 2001. Electrodynamic model of the lower atmosphere and the ionosphere coupling. Journal of Atmospheric and Solar-Terrestrial Physics 63 (16), 1681–1691.

Sorokin, V.M., Chmyrev, V.M., Yaschenko, A.K., 2003. Ionospheric generation mechanism of geomagnetic pulsations observed on the Earth's surface before earthquake. Journal of Atmospheric and Solar-Terrestrial Physics 65 (1), 21–29.

Sorokin, V.M., Chmyrev, V.M., Yaschenko, A.K., 2005a. Theoretical model of DC electric field formation in the ionosphere stimulated by seismic activity. Journal of Atmospheric and Solar-Terrestrial Physics 67 (14), 1259–1268.

Sorokin, V.M., Isaev, N.V., Yaschenko, A.K., Chmyrev, V.M., Hayakawa, M., 2005b. Strong DC electric field formation in the low latitude ionosphere over typhoons. Journal of Atmospheric and Solar-Terrestrial Physics 67 (14), 1269–1279.